

## 1 Cation-Dependent Self-assembly of Vanadium Polyoxoniobates

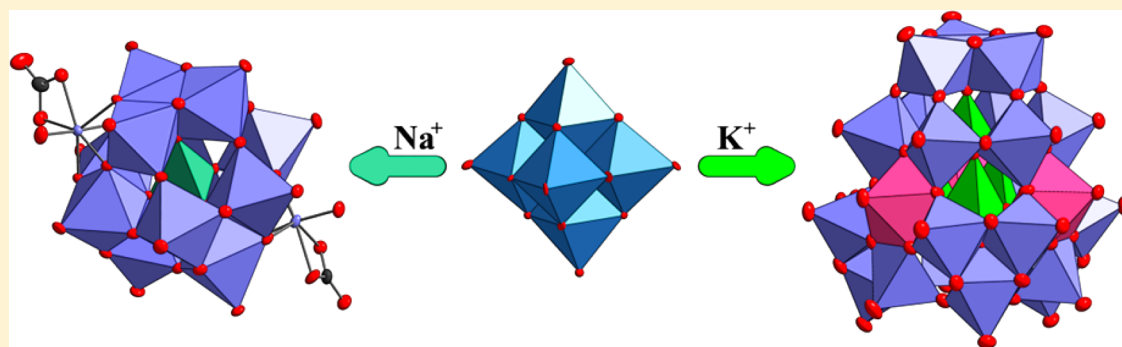
2 Pavel A. Abramov,<sup>\*,†,‡,§</sup> Anastasiia T. Davletgildeeva,<sup>†,‡</sup> Nikolay K. Moroz,<sup>†</sup> Nikolay B. Kompankov,<sup>†</sup>  
3 Beatrix Santiago-Schübel,<sup>§</sup> and Maxim N. Sokolov<sup>†,‡</sup>

4 <sup>†</sup>Nikolaev Institute of Inorganic Chemistry SB RAS, Novosibirsk, Russia 630090

5 <sup>‡</sup>Novosibirsk State University, Novosibirsk, Russia 630090

6 <sup>§</sup>Central Institute for Engineering, Electronics and Analytics – ZEA-3, Forschungszentrum Jülich, 52425, Jülich, Germany

7 **S** Supporting Information



8 **ABSTRACT:** Reaction of  $\text{Na}_7\text{H}[\text{Nb}_6\text{O}_{19}] \cdot 15\text{H}_2\text{O}$  with  $\text{NaVO}_3 \cdot 2\text{H}_2\text{O}$  at 220 °C in the presence of  $\text{NaHCO}_3$  gives new bicapped  
9  $\alpha$ -Keggin vanadododecaniobate  $[\text{VNb}_{12}\text{O}_{40}\{\text{NbO}(\text{CO}_3)\}_2]^{13-}$ , isolated and structurally characterized as  $\text{Na}_9\text{H}_4[\text{VNb}_{12}\text{O}_{40}-$   
10  $\{\text{NbO}(\text{CO}_3)\}_2] \cdot 37\text{H}_2\text{O}$  (**1**). According to  $^{51}\text{V}$  NMR and ESI-MS data, this anion equilibrates in solution with  $[\text{VNb}_{12}\text{O}_{40}]^{15-}$   
11 and oligomeric species that result from dissociation of the  $\{\text{NbO}(\text{CO}_3)\}^+$  fragments. In the presence of potassium, the same  
12 reaction gives  $[\text{V}_x\text{Nb}_{24}\text{O}_{76}]^{n-}$  ( $x = 4, n = 12$  (**2a**);  $x = 3, n = 17$  (**2b**)). The anions with  $x = 3$  and 4 cocrystallize together, but  
13 exist as separate entities both in solid and in solution according to  $^{51}\text{V}$  MASS NMR and ESI-MS data.

## 14 INTRODUCTION

15 The chemistry of niobium polyoxocomplexes (polyoxoniobates,  
16 PONb) is a challenging area of polyoxometalate chemistry,  
17 experiencing a spectacular renaissance.<sup>1</sup> Besides unique solution  
18 behavior defined by extraordinary strong cation association, the  
19 PONb show photocatalytic activity in water splitting,<sup>2</sup> which  
20 constitutes a hot topic in modern chemistry.<sup>3</sup> One of the  
21 problems in the chemistry of PONb is finding conditions for  
22 producing of larger, nanosized polyoxocomplexes—nanosized  
23 models of  $\text{Nb}_2\text{O}_5$ . The most common way to achieve this is  
24 thermal induction of the PONb aggregation from hexaniobates  
25  $[\text{Nb}_6\text{O}_{19}]^{8-}$  at different pHs. In this way, transient  $\{\text{Nb}_7\text{O}_{22}\}^{9-}$   
26 building blocks are generated, which combine into trimeric  
27  $[\text{Nb}_{24}\text{O}_{72}]^{14-}$  or larger aggregates.<sup>4</sup> Cronin et al. studied this  
28 aggregation in solutions of  $\text{K}_7\text{H}[\text{Nb}_6\text{O}_{19}] \cdot 13\text{H}_2\text{O}$  at 200 °C and  
29 were able to detect the formation of larger  $\{\text{Nb}_{10}\}$ ,  $\{\text{Nb}_{20}\}$ , and  
30  $\{\text{Nb}_{27}\}$  isopolyniobates, and isolate  $[\text{HNb}_{27}\text{O}_{76}]^{16-}$  and  
31  $[\text{H}_{10}\text{Nb}_{31}\text{O}_{93}(\text{CO}_3)]^{23-}$ .<sup>5</sup> Both complexes contain a rare  
32 pentagonal  $\{(\text{Nb})\text{Nb}_5\}$  building block, which had been  
33 observed only in Nb oxides.<sup>6</sup> The existence of such a unit  
34 indicates a link to the chemistry of giant polymolybdates, where  
35 the pentagonal  $\{(\text{Mo})\text{Mo}_5\}$  building blocks steer aggregation  
36 toward spherical and wheel-shaped nanoscale POMs like Mo  
37 blues or keplerates.<sup>7</sup> In the structure of  $[\text{HNb}_{27}\text{O}_{76}]^{16-}$ , there  
38 are four tetrahedral cavities inside the backbone, and a large

crown-ether like cavity in the bottom part. This means that 39  
heteroatoms with stable tetrahedral arrangements ( $\text{V}^{\text{V}}$ ,  $\text{P}^{\text{V}}$ ,  $\text{As}^{\text{V}}$ ) 40  
could stabilize such structures. Vanadium and phosphorus are 41  
the most suitable to prove this suggestion experimentally, both 42  
from their smaller size and amenability to NMR studies. In this 43  
contribution, we report hydrothermal rearrangements of 44  
sodium and potassium hexaniobates in the presence of 45  
 $\text{NaVO}_3$  as vanadium source, leading to vanadoniobates of two 46  
distinct types. 47

## 48 EXPERIMENTAL SECTION

**General Information.** Starting hexaniobates  $\text{A}_7\text{H}[\text{Nb}_6\text{O}_{19}] \cdot n\text{H}_2\text{O}$  49  
( $\text{A} = \text{Na}$ ,  $n = 15$ ;  $\text{A} = \text{K}$ ,  $n = 13$ ) were prepared according to the 50  
published procedures.<sup>8</sup> TG experiments were done on a NETZSCH 51  
TG 209 F1 device in an  $\text{Al}_2\text{O}_3$  crucible by heating a sample from 22 to 52  
300 °C with a 10 °C gradient. IR spectra ( $4000\text{--}400\text{ cm}^{-1}$ ) were 53  
recorded on a Vertex 80 spectrometer. Raman spectra ( $60\text{--}4000$  54  
 $\text{cm}^{-1}$ ) were obtained on a Triplemate spectrometer (Spex, USA) 55  
equipped with a multichannel detector LN-1340 PB (Princeton 56  
Instruments, USA). EDX analysis was performed on a HITACHI TM 57  
3000 Tabletop Microscope. Elemental analysis for **1** and **2** was carried 58  
out on a high-resolution spectrometer iCAP-6500 (Thermo Scientific) 59  
with a cyclone type spray chamber and “SeaSpray” nebulizer. NMR 60

**Received:** August 31, 2016

61 spectra were run on a Bruker Avance III 500 spectrometer at room  
62 temperature with addition of a very small amount of D<sub>2</sub>O to the  
63 sample aqueous solutions. The <sup>51</sup>V chemical shift was referenced to  
64 external VOCl<sub>3</sub> ( $\delta = 0$  ppm) as standard. The total sweep covered  
65 from  $-1000$  to  $0$  ppm. Solid state NMR experiments were run on a  
66 Bruker Avance III 500 spectrometer at  $5-15$  kHz.

67 **Synthesis of Na<sub>9</sub>H<sub>4</sub>[VNB<sub>12</sub>O<sub>40</sub>{NbO(CO<sub>3</sub>)<sub>2</sub>}]·37H<sub>2</sub>O (1).** Solid  
68 Na<sub>7</sub>H[Nb<sub>6</sub>O<sub>19</sub>]·15H<sub>2</sub>O (0.400 g, 0.31 mmol), NaVO<sub>3</sub>·2H<sub>2</sub>O (0.046 g,  
69 0.31 mmol), and NaHCO<sub>3</sub> (0.150 g, 1.79 mmol) were dissolved in 10  
70 mL of distilled water upon heating and stirring (pH 13.0). The  
71 solution was transferred into a stainless steel autoclave (the volume of  
72 the Teflon cartridge was 30 mL), and the mixture was kept at 220 °C  
73 for 18 h. After cooling, a colorless precipitate was filtered off (final pH  
74 was 10.3), and the filtrate was reduced in volume by heating at 90 °C  
75 to 3 mL. The concentrated solution was placed into a vial for slow  
76 evaporation. Rhombohedral colorless crystals were collected by  
77 filtration, rinsed with deionized water, and dried in air. Recrystalliza-  
78 tion from deionized water gave colorless crystals of 1. Yield 0.131 g  
79 (13%) based on niobium. EDX: atomic ratio Na:Nb:V = 9.1:13.8:1.0.  
80 ICP-AES found Na, Nb, V (%): 6.7, 43.6, 1.5, calculated for 1: Na, Nb,  
81 V (%): 6.9, 43.8, 1.7. <sup>51</sup>V NMR (H<sub>2</sub>O + D<sub>2</sub>O, r.t.,  $\delta$ , ppm):  $-481.3$ ;  
82  $-487.1$ ;  $-492.8$ ;  $-532.1$ . <sup>51</sup>V MASS NMR:  $-530$  ppm. <sup>13</sup>C MASS  
83 NMR:  $-166$  ppm. IR (KBr,  $\nu$ , cm<sup>-1</sup>): 3418 (s), 1604 (m), 1459 (m),  
84 1340 (m), 1053 (w), 874 (s), 800 (s), 656 (s), 581 (s), 461 (s), 401  
85 (s). Raman ( $\nu$ , cm<sup>-1</sup>): 1065 (m), 913(vs), 856(s), 368 (m), 250(m),  
86 215 (m). TGA: weight loss 13% corresponds to the removal of 30  
87 water molecules.

88 **Synthesis of 2, Containing Potassium Salts of [Nb<sub>24</sub>O<sub>76</sub>V<sub>4</sub>]<sup>12-</sup>**  
89 **(2a) and [V<sub>3</sub>Nb<sub>24</sub>O<sub>76</sub>]<sup>17-</sup> (2b).** Solid K<sub>7</sub>H[Nb<sub>6</sub>O<sub>19</sub>]·13H<sub>2</sub>O (0.400 g,  
90 0.30 mmol), NaVO<sub>3</sub>·2H<sub>2</sub>O (0.046 g, 0.31 mmol), and NaHCO<sub>3</sub>  
91 (0.150 g, 1.79 mmol) were dissolved in 10 mL of water upon heating  
92 and stirring (pH 13.0). The final solution was transferred into a  
93 stainless steel autoclave (30 mL Teflon cartridge), and the mixture was  
94 kept at 220 °C for 18 h. After cooling, a colorless precipitate was  
95 filtered off (final pH was 10.3), and the filtrate was reduced by heating  
96 at 90 °C to 3 mL volume. This concentrated solution was placed into a  
97 vial and left for crystallization. Overnight, hexagonal plate colorless  
98 crystals appeared and were collected by filtration, rinsed with  
99 deionized water, and dried in air. Repeated recrystallizations from  
100 small amounts of deionized water produced hexagonal plates suitable  
101 for X-ray analysis. Yield of 2 0.07 g (4%) based on niobium. <sup>51</sup>V NMR  
102 (H<sub>2</sub>O + D<sub>2</sub>O, r.t.,  $\delta$ , ppm):  $-532.5$ . <sup>51</sup>V MASS NMR:  $-532$  (m).  
103 Raman ( $\nu$ , cm<sup>-1</sup>): 1065 (m), 935(vs), 919(s), 907(s), 867 (m), 647  
104 (m), 498 (m), 360 (m), 329 (m), 244 (m), 211 (m). TGA: weight loss  
105 16% that corresponds to removal of 42 water molecules. EDX: atomic  
106 ratio K:Na:Nb:V is 1.6:2.3:6.7:1. ICP-AES: found K, Na, Nb, V (%):  
107 4.4, 4.3, 46.2, 3.5, calculated for K<sub>6</sub>Na<sub>8.5</sub>[Nb<sub>24</sub>V<sub>3.5</sub>O<sub>76</sub>]·42H<sub>2</sub>O (as 0.5/  
108 0.5 mixture of 2a and 2b) K, Na, Nb, V (%): 4.9, 4.1, 46.4, 3.7.

109 **Electrospray Ionization Mass Spectrometry (ESI-MS).** The  
110 experiments were performed on a hybrid linear ion trap FTICR mass  
111 spectrometer LTQ-FT (Thermo Fisher Scientific, Bremen, Germany)  
112 equipped with a 7 T supra-conducting magnet by infusion. The mass  
113 spectrometer was first tuned and calibrated in the negative mode  
114 following the standard optimization procedure for all voltages and  
115 settings. The complex was dissolved in 80% H<sub>2</sub>O, and 20% methanol  
116 was added for ionization. The transfer capillary temperature was set at  
117 175 °C. Mass spectra were recorded in full scan from 200 to 2000 Da  
118 with a resolution of 100,000 at  $m/z$  400. The data were processed with  
119 the Xcalibur software version 2.1.

120 **X-ray Diffraction.** The diffraction data were collected at 150 K on  
121 a Bruker Apex Duo (for 1) and on an Xcalibur (Agilent Technologies)  
122 at 130 K (for 2) single crystal diffractometers with Mo K $\alpha$  radiation ( $\lambda$   
123 = 0.71073 Å) by doing  $\omega$  and  $\phi$  scans of narrow (0.5°) frames. The  
124 structures were solved by direct methods and refined with full-matrix  
125 least-squares treatment against  $|F|^2$  in anisotropic approximation with  
126 SHELX 2014/7<sup>9</sup> in the ShelXle program.<sup>10</sup> Absorption corrections  
127 were applied empirically with SADABS<sup>11</sup> and SCALE3 ABSPACK  
128 programs (CrysAlisPro 1.171.38.41 (Rigaku OD, 2015)). Crystallo-  
129 graphic data and refinement details for 1 and 2 are listed in Table S1,  
130 and main bond distances for 1 are listed in Table S2.

Crystals of 2 grow as aggregates of thin poorly diffracting hexagonal  
plates, and the XRD data collection was done from a twinned crystal  
that gave a mediocre  $R$  value. Composition of 2 was assigned with the  
help of EDX, TGA, and ESI-MS data.

Crystallographic data files for 1 and 2 have been deposited with  
ICSD (Fachinformationszentrum Karlsruhe, 76344 Eggenstein-Leo-  
poldshafen, Germany; e-mail: [crysdata@fz-karlsruhe.de](mailto:crysdata@fz-karlsruhe.de)) with num-  
bers CSD 431897 (1), CSD 431896 (2).

## RESULTS AND DISCUSSION

**Synthesis and Structure of 1.** Heating a mixture of 140  
sodium metavanadate and sodium hexaniobate at 220 °C 141  
(initial pH 12) for 18 h produces a copious amorphous material 142  
and a clear colorless solution, which contains two distinct types 143  
of vanadates, according to <sup>51</sup>V NMR data—mainly the cyclic 144  
tetravanadate [V<sub>4</sub>O<sub>12</sub>]<sup>4-</sup> (which is the dominant form of 145  
vanadate at  $C_v$  10<sup>-2</sup> M and pH 8–10;<sup>12</sup> the final pH dropped to 146  
10.3), together with a small amount of a new product. The 147  
controlled evaporation solution gave a tiny amount of 148  
hexagonal plates of Na<sub>9</sub>H<sub>4</sub>[VNB<sub>12</sub>O<sub>40</sub>{NbO(CO<sub>3</sub>)<sub>2</sub>}]·37H<sub>2</sub>O 149  
(1). The incorporation of carbonate was due to absorption of 150  
CO<sub>2</sub> from air by the strongly basic solution of hexaniobate. 151  
Consequently, addition of NaHCO<sub>3</sub> significantly improves the 152  
yield of 1 (up to 13%) and makes it possible to study its 153  
chemistry. 154

The vanadatotetrakaidekaniobate [VNB<sub>14</sub>O<sub>42</sub>(CO<sub>3</sub>)<sub>2</sub>]<sup>13-</sup> 155  
anion present in 1 (Figure 1) has an  $\alpha$ -Keggin-type structure 156

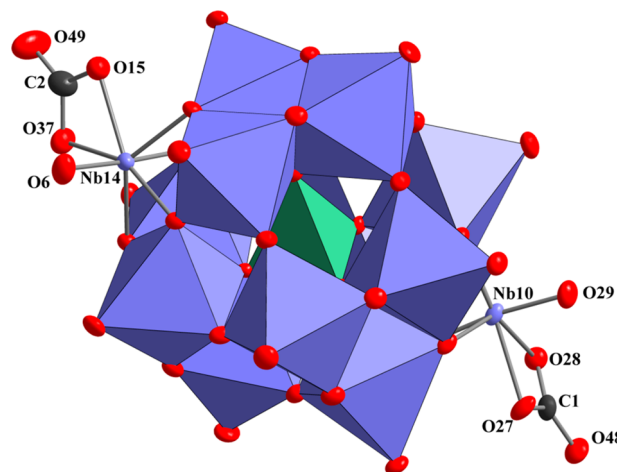


**Figure 1.** Structure of [VNB<sub>14</sub>O<sub>42</sub>(CO<sub>3</sub>)<sub>2</sub>]<sup>13-</sup> (thermal ellipsoids drawn with 50% probability). Main bond distances:  $d(\text{O6-Nb14}) = 1.772(7)$  Å;  $d(\text{O15-Nb14}) = 2.181(7)$  Å;  $d(\text{O37-Nb14}) = 2.149(7)$  Å;  $d(\text{O27-Nb10}) = 2.175(7)$  Å;  $d(\text{O28-Nb10}) = 2.170(6)$  Å;  $d(\text{O29-Nb10}) = 1.774(7)$  Å;  $d(\text{V-O})_{\text{av}} = 1.695(6)$  Å.

with two extra {NbO(CO<sub>3</sub>)<sup>+</sup>} caps, where the niobium atom 157  
has coordination number 7. BVS for oxygen atoms of CO<sub>3</sub><sup>2-</sup> 158  
(Table S3) agrees with partial protonation of O49. This mode 159  
of capping is typical for highly charged heterododekaniobates: 160  
in K<sub>12</sub>(Ti<sub>2</sub>O<sub>2</sub>)[SiNb<sub>12</sub>O<sub>40</sub>]·16H<sub>2</sub>O, the Keggin anions [SiNb<sub>12</sub>- 161  
O<sub>40</sub>]<sup>16-</sup> are capped by additional {TiO}<sup>2+</sup> groups which unite 162  
them into infinite chains.<sup>13</sup> In Na<sub>10</sub>(Nb<sub>2</sub>O<sub>2</sub>)[TNb<sub>12</sub>O<sub>40</sub>]·xH<sub>2</sub>O 163  
(T = Si, Ge), there are additional {NbO}<sup>3+</sup> caps with a similar 164  
function.<sup>14</sup> However, there are also uncapped dodekaniobates, 165  
as is the case of Na<sub>16</sub>[TNb<sub>12</sub>O<sub>40</sub>]·4H<sub>2</sub>O (T = Si, Ge).<sup>15</sup> Single 166  
capped germano- and silicododekaniobates, namely, Rb<sub>13</sub>- 167  
[GeNb<sub>13</sub>O<sub>41</sub>]·23H<sub>2</sub>O, Cs<sub>10.6</sub>[H<sub>2.4</sub>GeNb<sub>13</sub>O<sub>41</sub>]·27H<sub>2</sub>O, and 168  
Cs<sub>18</sub>H<sub>6</sub>[(NbOH)SiNb<sub>12</sub>O<sub>40</sub>]<sub>2</sub>·38H<sub>2</sub>O, were isolated.<sup>16</sup> Small 169

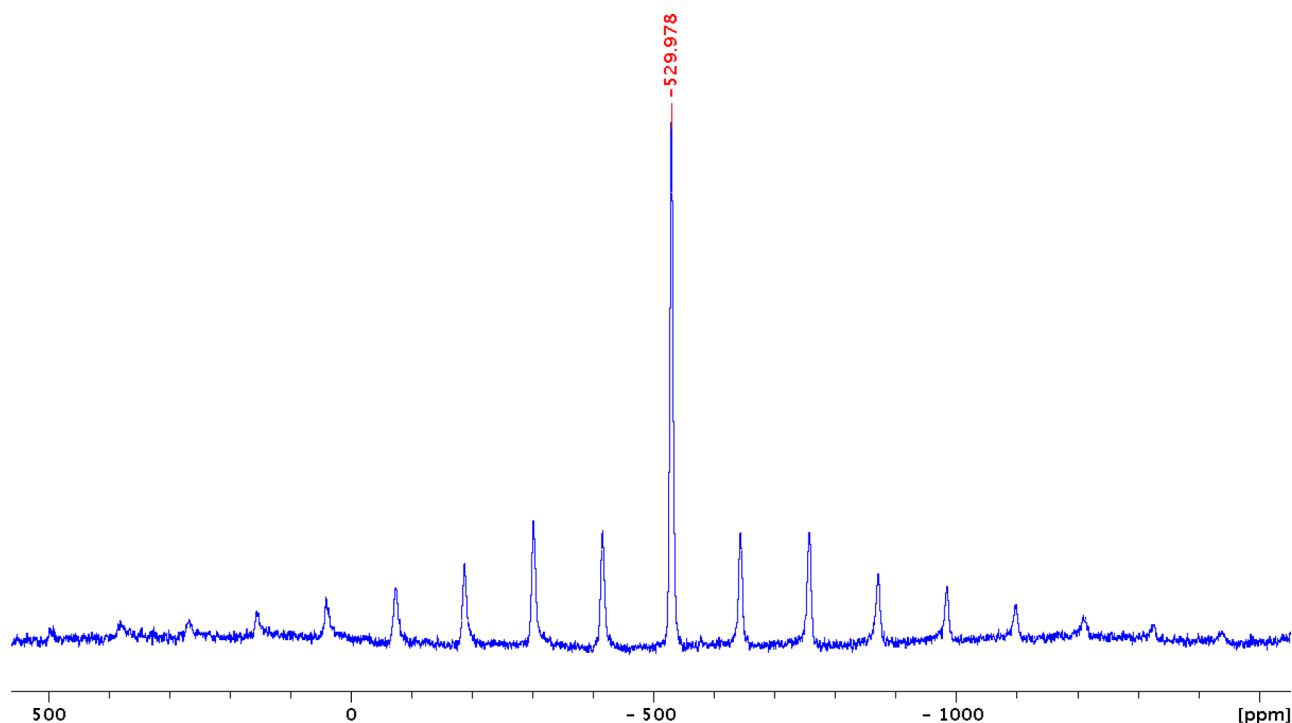


Figure 2.  $^{51}\text{V}$  MASS NMR spectrum of 1.

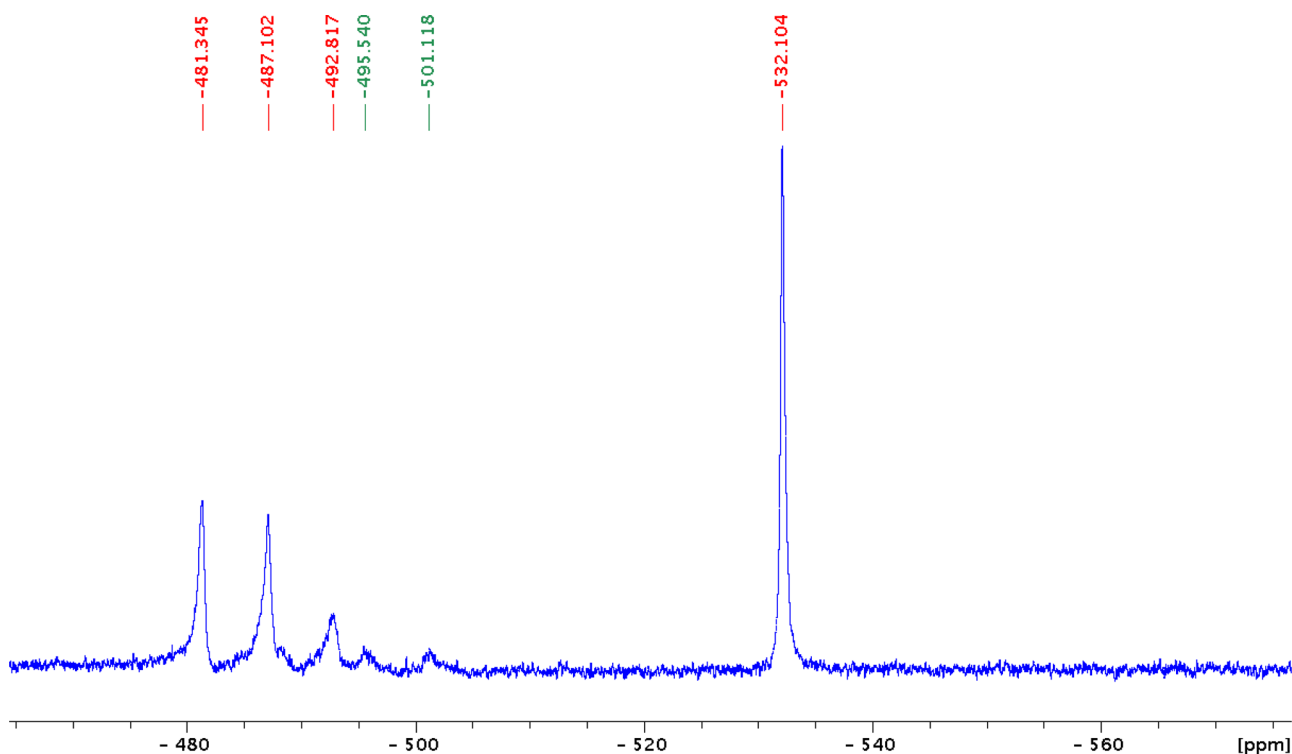
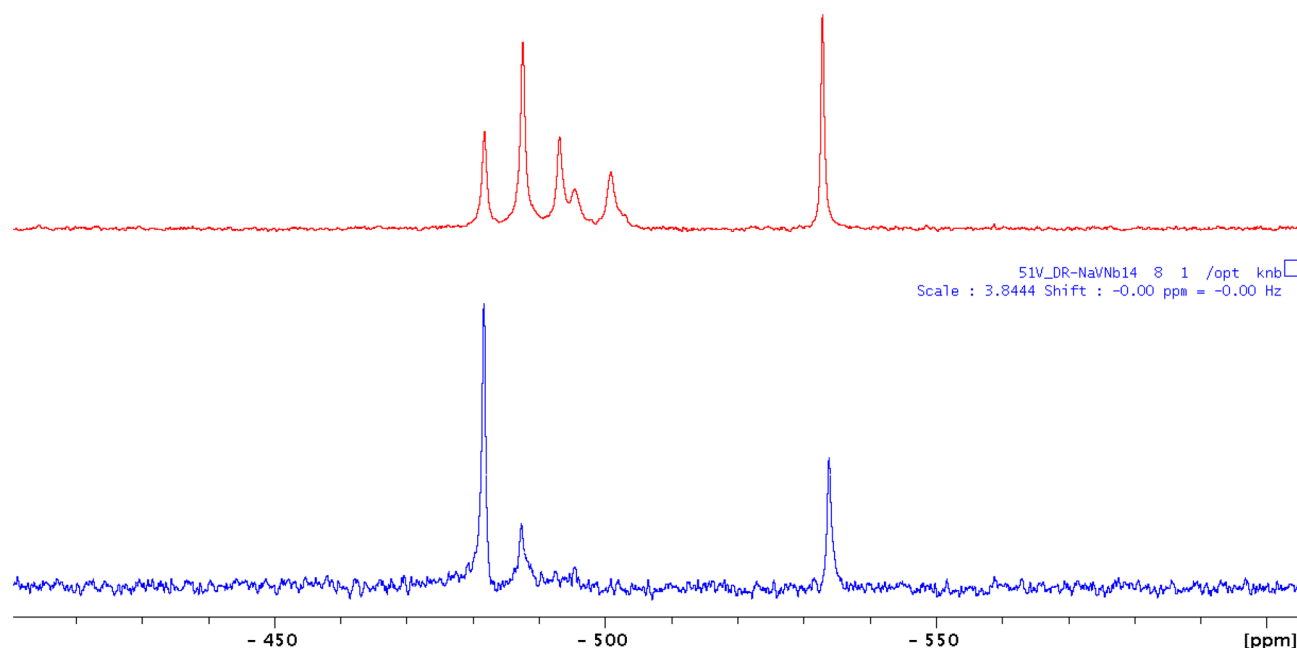


Figure 3.  $^{51}\text{V}$  NMR spectrum of the solution of 1 at natural pH.

angle X-ray scattering (SAXS) studies on the solutions of  $\text{Rb}_{13}[\text{GeNb}_{13}\text{O}_{41}] \cdot 23\text{H}_2\text{O}$  and  $\text{Cs}_{10.6}[\text{H}_{2.4}\text{GeNb}_{13}\text{O}_{41}] \cdot 27\text{H}_2\text{O}$  revealed oligomerization of the monomers into the chain structures through the dimerization of the  $\{\text{NbO}\}^{3+}$  caps. The extent of the oligomerization is controlled by pH, concentration, and the counterion, and chains built of up to six Keggin links with large were observed in the presence of large alkali metal cations. In our case, the polymerization of the

$[\text{VNb}_{12}\text{O}_{40}\{\text{NbO}\}_2]^{10-}$  bicapped Keggin anions is blocked by coordination of  $\text{CO}_3^{2-}$  to the coordinatively unsaturated capping Nb atoms (CN would be 5 without carbonate). The main bond distances in  $[\text{VNb}_{14}\text{O}_{42}(\text{CO}_3)_2]^{13-}$  are listed in Figure 1.

The lighter analogue of niobium—vanadium—also forms a similar bicapped Keggin anion  $[\text{PV}_{14}\text{O}_{42}]^{9-}$ , but under strongly acidic conditions.<sup>17</sup> Due to the smaller ionic radius of  $\text{V}^{5+}$ , it



**Figure 4.** Concentration dependence of  $^{51}\text{V}$  NMR signals in **1**. Upper spectrum recorded for 4.7 mM, lower for 0.8 mM aqueous solutions.

shows no tendency to polymerize into the chains and apparently exists only in the monomeric form. The  $\{\text{VO}\}^{n+}$  groups can also cap highly charged reduced dodecamolybdate Keggin anions, as in  $[\text{PMo}_{12}\text{O}_{40}(\text{VO})_2]^{n-18}$  or  $[\text{GeMo}_{12}\text{O}_{40}(\text{VO})_2]^{3-19}$ . The  $[\text{PMo}_{12}\text{O}_{40}(\text{VO})_2]^{n-}$  has been assessed as an important model for spin qubit because the redox-active core unit of the Keggin phosphomolybdate is capped on the opposed positions by two vanadyl ions (2+), each containing a localized spin of 1/2. These spins can be coupled through the electrons of the central core by electrical manipulation of the molecular redox potential owing to the change of charge.<sup>20</sup> The  $\{\text{VO}\}^{3+}$  caps can be coordinated to Keggin-type dodecaniobates in  $(\text{TMA})_9[\text{V}_3\text{Nb}_{12}\text{O}_{42}] \cdot 18\text{H}_2\text{O}$ <sup>21</sup> and  $[\text{Cu}(\text{en})_2]_{3.5}[\text{Cu}(\text{en})_2(\text{H}_2\text{O})]\{[\text{VNb}_{12}\text{O}_{40}(\text{VO})_2][\text{Cu}(\text{en})_2]\} \cdot 17\text{H}_2\text{O}$ .<sup>22</sup> In this way, they can even occupy up to six vertex positions, as in  $[\text{Cu}(\text{en})_2]_4[\text{PNb}_{12}\text{O}_{40}(\text{VO})_6](\text{OH})_5 \cdot 8\text{H}_2\text{O}$  and in  $[\text{Cu}(\text{enMe})_2]_4[\text{PNb}_{12}\text{O}_{40}(\text{VO})_6](\text{OH})_5 \cdot 6\text{H}_2\text{O}$  (en = 1,2-ethylenediamine and enMe = 1,2-diaminopropane).<sup>23</sup> In our case, we used a Nb:V = 6:1 atomic ratio and no vanadyl caps entered the structure. Reactions with larger vanadium-to-niobium molar ratios are under investigation.

Recently Su et al. reported preparations of  $[\text{Na}(\text{H}_2\text{en})_5][\text{VNb}_{14}\text{O}_{42}(\text{NO}_3)_2] \cdot 12\text{H}_2\text{O}$  and  $\text{K}_7\text{Na}_4[\text{VNb}_{14}\text{O}_{42}(\text{NO}_3)_2] \cdot 31\text{H}_2\text{O}$  by heating together  $\text{V}_2\text{O}_5$ , NaOH,  $\text{K}_7\text{H}[\text{Nb}_6\text{O}_{19}] \cdot 13\text{H}_2\text{O}$ ,  $\text{Co}(\text{NO}_3)_2 \cdot 6\text{H}_2\text{O}$ , and ethylenediamine.<sup>24</sup> We also tried to switch from carbonate to nitrate, but no  $[\text{VNb}_{14}\text{O}_{42}(\text{NO}_3)_2]^{13-}$  was detected. It means that, under conditions as used for preparation of **1**, weakly coordinating nitrate cannot stabilize the vanadododecaniobate structure.

**Solid State and Solution Studies of 1.** A crystalline sample of **1** was studied with  $^{51}\text{V}$  and  $^{13}\text{C}$  MASS NMR techniques (Figure 2). In the  $^{51}\text{V}$  spectrum, at a rotation speed of 15 kHz, a single line at  $-530$  ppm from the  $\{\text{VO}_4\}^{3-}$  moiety inside the bicapped Keggin was observed.

In  $^{13}\text{C}$  MASS NMR, we found one unsymmetrical signal at 166 ppm (15 kHz) resulting from nonequal orientations of the  $\text{CO}_3^{2-}$  ligands in the crystal structure (Figure S1). These data confirm the individuality of the crystalline sample of **1**.

However, dissolving **1** in water produces several species, according to  $^{51}\text{V}$  NMR data (Figure 3). The main solution signal at  $-532$  ppm corresponds to  $-530$  ppm assigned to the signal from the bicapped Keggin anion in solid state.

In order to identify the other signals, we probed the solutions of  $[\text{VNb}_{14}\text{O}_{42}(\text{CO}_3)_2]^{13-}$  with the ESI-MS technique (see Figure S1 and Table S4). We observed two series of signals, one from uncapped Keggin anions ( $[\text{VNb}_{12}\text{O}_{40} + n\text{Na}^+ + m\text{H}^+]^{2-}$ ) and the other from bicapped Keggin anions ( $[\text{VNb}_{12}\text{O}_{40} \cdot \{\text{NbO}(\text{CH}_3\text{O})_2\}_2 + x\text{Na}^+ + y\text{H}^+]^{2-}$ ), respectively. The substitution of a carbonate ligand with two methoxo ligands is due to the fact that the ESI-MS spectra were recorded essentially in methanol with a small amount of water added. Consequently, we have assigned the signals in the area between  $-480$  and  $-510$  ppm to these species. Taking into account the reported SAXS data on the solution behavior of  $[\text{GeNb}_{13}\text{O}_{41}]^{13-}$ , we have also to admit that some of these signals might correspond to oligomerization of the Keggin anions through  $\{\text{Nb}_2\text{O}_2\}$  bridges after the loss of carbonate.<sup>16</sup>

This oligomerization could not be detected under ESI-MS conditions since the concentration of the sample was below  $10^{-5}$  M, which was much lower than that used for recording  $^{51}\text{V}$  NMR. In order to get a more consistent picture, we have studied aqueous solutions of **1** with  $^{51}\text{V}$  NMR by varying the concentration, and indeed found that several of these additional signals decrease at lower concentrations (Figure 4). This is consistent with the dissociation of oligomeric species. At the same time, the relative intensity of the signal at  $-482$  ppm significantly increases with dilution, while that of the parent  $[\text{VNb}_{14}\text{O}_{42}(\text{CO}_3)_2]^{13-}$  anion at  $-532$  ppm simultaneously decreases. This can be explained by reversible dissociation of the  $\{\text{NbO}\}^{3+}$  caps being favored in diluted solutions.

This experiment fixes the signal from the noncapped Keggin form  $[\text{VNb}_{12}\text{O}_{40}]^{15-}$  to  $-482$  ppm. Moreover, as a single-capped link between  $[\text{VNb}_{12}\text{O}_{40}]^{15-}$  and  $[\text{VNb}_{14}\text{O}_{42}(\text{CO}_3)_2]^{13-}$ , we have to admit the existence of a dimer  $\{[\text{Nb}_2\text{O}_2][\text{VNb}_{12}\text{O}_{40}]_2\}$ .<sup>24</sup> If this is correct, the signal at  $-487$  ppm can be assigned to this species.



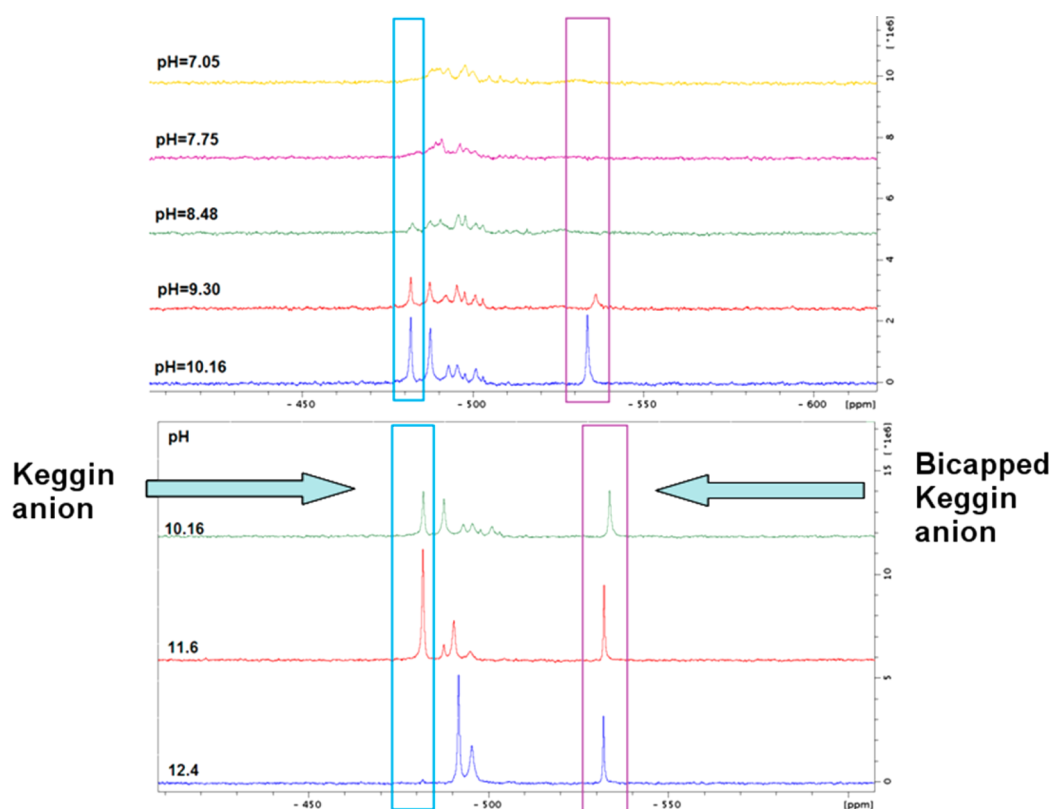


**Figure 5.** Dependence of  $^{51}\text{V}$  NMR signals of **1** from pH value.

We have run  $^{51}\text{V}$  NMR experiments at various pHs and found that the relative stabilities of the capped and noncapped Keggin ions are pH-dependent (Figure 5).

From these data, we can estimate the pH stability windows for  $[\text{VNB}_{12}\text{O}_{40}]^{15-}$  and  $[\text{VNB}_{14}\text{O}_{42}(\text{CO}_3)_2]^{13-}$  as being  $11.6 \div 8.4$  and  $13 \div 9.2$  pH units, respectively. At  $\text{pH} \geq 12.4$ ,  $[\text{VNB}_{12}\text{O}_{40}]^{15-}$  is not detected, but the intensities of the  $-492$  and  $-496$  ppm peaks increase. This can be attributed to the formation of the single-capped Keggin anion  $[\text{VNB}_{12}\text{O}_{40}(\text{NbO}(\text{CO}_3))]^{14-}$ . Moreover, gradually reducing the pH value to 7 gives rise to an additional number of peaks clustering between  $-480$  and  $-510$  ppm, in accordance with the formation of  $(\text{Nb}_2\text{O}_2)$ -bridged oligomers. Finally, at pH 7, we observe only these oligomeric forms. Remarkably, no free vanadate species were detected in all of these experiments, indicating the preservation of the Keggin structure within the investigated pH window.

We could not find reference  $^{51}\text{V}$  NMR data for “trans-vanadium” bicapped Keggin-type complexes  $\{\text{VNB}_{12}\text{O}_{40}(\text{VO})_2\}$ ,<sup>22</sup> nor are  $^{51}\text{V}$  MASS NMR data available for  $[\text{Na}(\text{H}_2\text{en})_5][\text{VNB}_{14}\text{O}_{42}(\text{NO}_3)_2] \cdot 12\text{H}_2\text{O}$  and  $\text{K}_7\text{Na}_4[\text{VNB}_{14}\text{O}_{42}(\text{NO}_3)_2] \cdot 31\text{H}_2\text{O}$ .<sup>24</sup> However,  $^{51}\text{V}$  NMR spectra of  $(\text{TMA})_9[\text{V}_3\text{Nb}_{12}\text{O}_{42}] \cdot 18\text{H}_2\text{O}$  exhibited a sharp peak at  $-520.0$  ppm and a broad peak at  $-528.1$  ppm with an approximate integrated intensity ratio of 1:2, corresponding to a central  $\text{VO}_4$  and two capping  $\{\text{VO}\}$  units in the cluster.<sup>21</sup> Given the quadrupolar nature of  $^{51}\text{V}$ , a reasonable hypothesis would be to assign the sharp signal to the symmetric  $\text{VO}_4$ , and the broader peak at  $-528.1$  ppm to the less-symmetric capping  $\text{VO}_5$  sites. This assignment agrees well with the  $^{51}\text{V}$  NMR studies of isostructural bicapped Keggin isopolyoxovanadate,  $[\text{VV}_{12}\text{O}_{40}(\text{VO})_2]^{9-}$ , for which the signal from the central  $\text{VO}_4$  was observed at  $-507$  ppm, and  $\text{VO}_5$  appeared at  $-531$  ppm.<sup>25</sup>

Furthermore, for  $[\text{PV}_{12}\text{O}_{40}(\text{VO})_2]^{9-}$ , the  $-523$  ppm peak was assigned to the  $\text{VO}_5$  caps, and the  $-575$  ppm peak to the  $\text{VO}_6$  addenda.<sup>17</sup>

**Isolation and Structure of 2.** The chemistry of polyoxoniobates and tantalates is strongly influenced by the counterions. Aggregation of Lindqvist-type hexametalates with cations both in solid state and in solution is well documented.<sup>1a</sup> Applying these considerations to higher-nuclearity PONb, we have compared the products formed by heating hexaniobate with vanadate: (i) in the presence of sodium solely and (ii) in the presence of potassium and sodium. The pure  $\text{Na}^+$  salts yielded **1**, while, in the presence of  $\text{K}^+$ , after carefully monitored evaporation of the filtrate from the reaction mixture, we obtained crystals containing  $[\text{K}@\text{V}_x\text{Nb}_{24}\text{O}_{76}]^{n-}$  (**2**) displaying a hitherto unprecedented anion structure (Figure 6).

The anion is built of three edge-sharing  $\{\text{NbO}_6\}$  octahedra having common vertices with three fused  $\{(\text{NbO}_2)(\text{NbO}_6)_5\}$  pentagonal units, which, in turn, are additionally bridged with three *trans*- $\{\text{NbO}_2\}$  fragments, all forming the polyoxoniobate backbone. Alternatively, the structure can be regarded as a hybrid of a trilacunary  $\{\text{VNB}_9\}$  Keggin anion and a polyniobate based on corner-shared pentagonal  $\{\text{NbNb}_5\}$  units, as found, e.g., in the hexatriakontamolybdate  $[\text{Mo}_{36}\text{O}_{112}(\text{H}_2\text{O})_{16}]^{8-}$ .<sup>7</sup> This particular combination is apparently without precedents in the chemistry of polyoxomolybdates. There are five cavities inside the anion: four pseudotetrahedral T-cavities (with four short ( $1.829\text{--}2.088$  Å) and two long ( $2.395\text{--}2.434$  Å) V–O distances) inside, and a large crown-ether like lacuna at the bottom part. The T-cavities are occupied with vanadium with either full or  $3/4$  occupancy, and the large lacuna accommodates a single  $\text{K}^+$  cation (Figure S2). These four T-cavities form a supertetrahedral cavity with the topology of the  $\text{P}_4\text{O}_{10}$  cage.

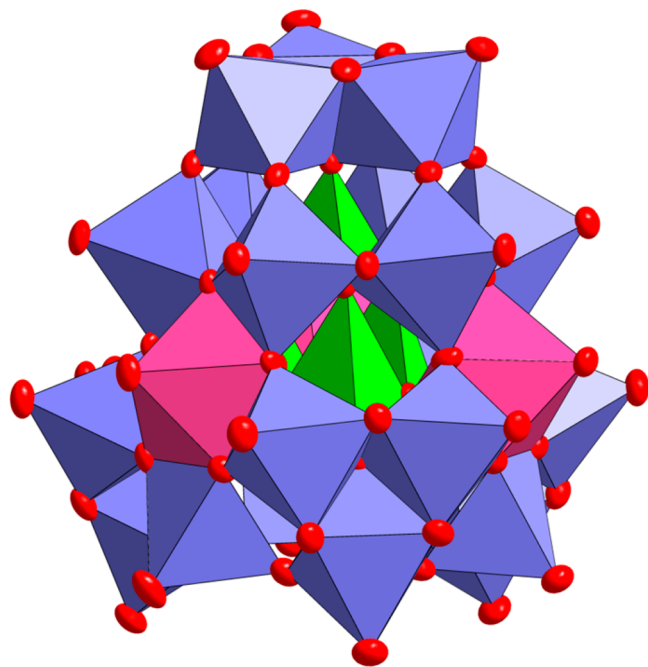


**Figure 6.** View of  $[\text{V}_x\text{Nb}_{24}\text{O}_{76}]^{n-}$  (combined ellipsoid (50% probability) and polyhedral model). Vanadium polyhedra are shown in green, niobium polyhedra with CN 7 in pink.

the case of Nb, the coordination can be described as a highly distorted tetrahedron with two additionally coordinated oxides. Such an arrangement was found only in the rare-earth orthoniobates  $\text{LnNbO}_4$  (Fergusonite-type mineral), which can also be synthesized at the temperature range between 500 and 1100 °C.<sup>26</sup> Accordingly to the neutron diffraction experiments, the Nb–O distances in such a tetrahedron are 1.834 Å.<sup>27</sup> Recently, Kolis et al. also reported about the synthesis of rare earth orthoniobates  $\text{RENbO}_4$  (RE = Y, La–Lu).<sup>28</sup>

These compounds were grown as large single crystals in 30 M KOH at 700 °C and 2 kbar. Niobium occupies a 4e Wyckoff position having 2-fold symmetry and forms shorter bonds to four oxygen atoms with a narrow spread of distances (average Nb–O distances of 1.846(5) and 1.927(5) Å across the  $\text{RENbO}_4$  family) and much longer bonds to two other oxygen atoms (average Nb–O distance of 2.455(5) Å) to form the distorted  $\text{NbO}_6$  unit. It seems not very likely that already at 200 °C niobium would spontaneously enter such energetically disfavored positions. A kind of a structural artifact arising from the disorder is not to be discarded, and perhaps the Nb occupancies of the T-cavities in  $[\text{HNb}_{27}\text{O}_{76}]^{16-}$  should, in fact, be less than 1, if not zero. Unfortunately, we also have encountered severe problems with crystal diffraction in **2** due to the formation of stacks of poorly diffracting very thin plates.

It is also interesting that, in the presence of roughly equimolar amounts of  $\text{K}^+$  (2.17 mmol) and  $\text{Na}^+$  (1.90 mmol) used in the preparation of **2**, it is exclusively potassium that enters the lacuna. If one compares the cation-accommodating lacuna in **2** with what is found in other polyniobates, one can cite  $[\text{K}@\text{Nb}_{24}\text{O}_{72}\text{H}_9]^{14-}$ , which has a very similar crown-ether like cavity flanked by six  $\{\text{NbO}_6\}$  fragments. Moreover, such a cyclic structure occurs in a pyrochlore mineral  $(\text{Na,Ca})_2\text{Nb}_2\text{O}_6(\text{OH,F})$ .<sup>29</sup> Hence, we can suggest that this cyclic arrangement  $\{\text{K}@\text{NbO}_6\}$  is energetically preferred at higher temperatures and can be generated and used as a building block for construction of various polyniobates.

Looking across the periodic table for structural analogues of **2**, we have found structures of  $[\text{H}_2\text{Ti}_{28}\text{O}_{38}(\text{OEt})_{40}\text{LnCl}]$  (Ln = La, Ce) with a closely related metal core, which also contain three pentagonal  $\{(\text{Ti})\text{Ti}_5\}$  building blocks, and has a large cavity flanked with six  $\{\text{TiO}_6\}$  octahedra, occupied with a  $\text{Ln}^{3+}$  cation.<sup>30</sup> It is yet another example of the diagonal relationship between niobium and titanium.

**Solid State and Solution Studies of 2.** The solubility of **2** in water is practically the same as of  $\text{KVO}_3$ , which makes

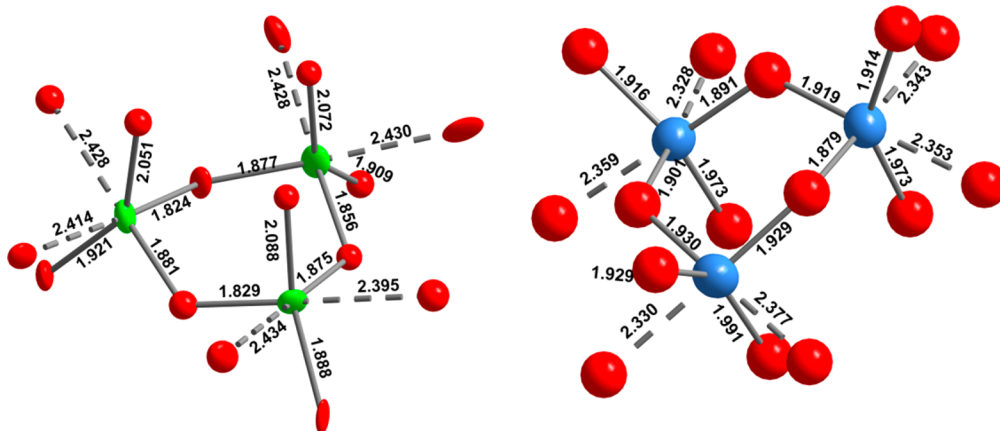


**Figure 7.** Comparison of the T-cavities geometry in **2** (left) and in CSD 420848 (right).

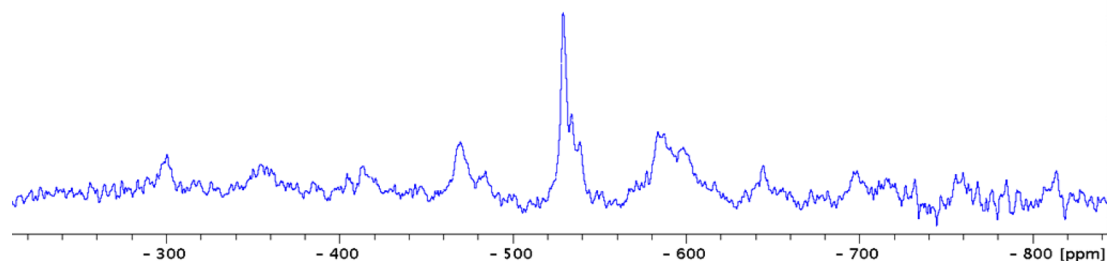


**Figure 8.**  $^{51}\text{V}$  MASS NMR for **2**. Intensity of satellites is low due to low content of **2** (mixed with  $\text{SiO}_2$ ).

fractional crystallization of this complex very complicated, and the purity of the bulk product does not allow exact determination of the analytical composition. Moreover, the simultaneous presence of two anions in the single crystal phase turns fitting analytical data unequivocally into a very difficult task. We studied solutions of several crystals of **2**, picked up manually, with ESI-MS, and always found two overlapping series of anions:  $[\text{CH}_3\text{OH} + \text{V}_4\text{Nb}_{24}\text{O}_{76} + x\text{K} + y\text{H}]^{3-}$ ,  $[\text{H}_2\text{O} + \text{V}_4\text{Nb}_{24}\text{O}_{76} + x\text{Na} + y\text{H}]^{3-}$ ,  $[\text{H}_2\text{O} + \text{V}_3\text{Nb}_{24}\text{O}_{76} + x\text{K} + y\text{H}]^{3-}$ ,  $[\text{CH}_3\text{OH} + \text{V}_3\text{Nb}_{24}\text{O}_{76} + x\text{K} + y\text{H}]^{3-}$ ,  $[\text{H}_2\text{O} + \text{V}_3\text{Nb}_{24}\text{O}_{76} + x\text{Na} + y\text{H}]^{3-}$  (see Table S5, Figure S4). These data confirm the individuality of  $[\text{V}_4\text{Nb}_{24}\text{O}_{76}]^{12-}$  and  $[\text{V}_3\text{Nb}_{24}\text{O}_{76}]^{17-}$  present in **2**.

In the  $^{51}\text{V}$  MASS NMR, there is a set of signals centered at  $-530$  ppm (Figure 8). In solution, they merge into a single line at  $-532$  ppm (150 Hz width), due to the quadrupolar nature of the  $^{51}\text{V}$  nucleus.

In the Raman spectra of **1** and **2**, there are sets of Nb–O and V–O vibrations (Figure S5): 1065 (m), 913(vs), 856(s), 368 (m), 250(m), 215 (m) for **1** and 1065 (m), 935(vs), 919(s), 907(s), 867 (m), 647 (m), 498 (m), 360 (m), 329 (m), 244 (m), 211 (m) for **2**. The bands at  $1065\text{ cm}^{-1}$  can be assigned to the tetrahedral  $\text{VO}_4$  units. The strong bands at 913 (**1**) and 935 (**2**)  $\text{cm}^{-1}$  should correspond to terminal Nb=O groups. The Nb–O–Nb bridges appear below  $900\text{ cm}^{-1}$ , as can be expected from the comparison with the Raman spectra of  $\text{ANbO}_3$  (the highest frequency Nb–O bands at  $876\text{ cm}^{-1}$  (for  $\text{Li}^+$ ),  $800\text{ cm}^{-1}$  (for  $\text{Na}^+$ ),  $832\text{ cm}^{-1}$  (for  $\text{K}^+$ )).<sup>31</sup> In  $\text{CaNb}_2\text{O}_6$ , the Nb–O band appears at  $904\text{ cm}^{-1}$ , and in  $\text{AlNbO}_4$  at  $932\text{ cm}^{-1}$ .<sup>31</sup>

## CONCLUSION

This research demonstrates rich synthetic possibilities of thermal rearrangements of hexaniobate, which, depending on the cationic composition of the reaction mixture, can follow different pathways. In the case of sodium, we isolated  $\text{Na}_9\text{H}_4[\text{VNb}_{12}\text{O}_{40}\{\text{NbO}(\text{CO}_3)\}_2] \cdot 34\text{H}_2\text{O}$  consisting of a bicapped  $\alpha$ -Keggin-type V-centered polyoxoniobate. In water, it equilibrates with vanadododecaniobate and polymeric forms by a process involving the loss of coordinated carbonate, one or two  $\{\text{NbO}\}^{3+}$  caps, and oligomerization by their transformation into  $\{\text{Nb}_2\text{O}_2\}^{6+}$  linkers. In the presence of potassium, we isolated a solid phase containing two unique  $[\text{V}_4\text{Nb}_{24}\text{O}_{76}]^{12-}$  and  $[\text{V}_3\text{Nb}_{24}\text{O}_{76}]^{17-}$  anions with the topology of a trigonal pyramid. These PONb have a hybrid metal-oxo backbone consisting of a fragment of the Keggin structure fused with pentagonal  $\{\text{NbNb}_3\}$  building blocks, arranged around a central tetrahedral cavity. The cavity is occupied by three or four  $\text{V}^{5+}$  ions. In this way,  $[\text{V}_4\text{Nb}_{24}\text{O}_{76}]^{12-}$  can be regarded as a polyniobate assembled around  $\text{V}_4\text{O}_{10}$  as template—a molecular analogue of  $\text{P}_4\text{O}_{10}$ , unknown in the free state, but stabilized

when trapped into PONb.  $[\text{V}_3\text{Nb}_{24}\text{O}_{76}]^{17-}$  can be similarly regarded as incorporating cyclic trivanadate  $[\text{V}_3\text{O}_9]^{3-}$ , which has negligible contribution to the equilibria in the solutions of free vanadates. In this work, we have also demonstrated remarkable tendency of a cyclic  $\{\text{K}@\text{(NbO}_6)_6\}$  building block to assemble at higher temperatures.

## ASSOCIATED CONTENT

### Supporting Information

The Supporting Information is available free of charge on the ACS Publications website at DOI: 10.1021/acs.inorgchem.6b02108.

Additional structural information, ESI(–)-MS data, and

Raman spectra (PDF)

Crystallographic data for **1** (CIF)

Crystallographic data for **2** (CIF)

## AUTHOR INFORMATION

### Corresponding Author

\*E-mail: [abramov@niic.nsc.ru](mailto:abramov@niic.nsc.ru).

### ORCID

Pavel A. Abramov: 0000-0003-4479-5100

### Funding

The work was supported by the Russian Science Foundation (RScF 14-13-00645).

### Notes

The authors declare no competing financial interest.

## REFERENCES

- (1) (a) Nyman, M. Polyoxoniobate chemistry in the 21st century. *Dalton Trans.* **2011**, 40, 8049–8058. (b) Kinnan, M. K.; Creasy, W. R.; Fullmer, L. B.; Schreuder-Gibson, H. L.; Nyman, M. Nerve Agent Degradation with Polyoxoniobates. *Eur. J. Inorg. Chem.* **2014**, 2014, 2361–2367. (c) Abramov, P. A.; Vicent, C.; Kompankov, N. B.; Gushchin, A. L.; Sokolov, M. N. Platinum polyoxoniobates. *Chem. Commun.* **2015**, 51, 4021–4023. (d) Abramov, P. A.; Sokolov, M. N.; Virovets, A. V.; Floquet, S.; Haouas, M.; Taulelle, F.; Cadot, E.; Vicent, C.; Fedin, V. P. Grafting  $\{\text{Cp}^*\text{Rh}\}^{2+}$  on the surface of Nb and Ta Lindqvist-type POM. *Dalton Trans.* **2015**, 44, 2234–2239. (e) Son, J.-H.; Wang, J.; Casey, W. H. Structure, stability and photocatalytic  $\text{H}_2$  production by Cr-, Mn-, Fe-, Co-, and Ni-substituted decaniobate clusters. *Dalton Trans.* **2014**, 43, 17928–17933.
- (2) (a) Huang, P.; Qin, C.; Su, Z.-M.; Xing, Y.; Wang, X.-L.; Shao, K.-Z.; Lan, Y.-Q.; Wang, E.-B. Self-Assembly and Photocatalytic Properties of Polyoxoniobates:  $\{\text{Nb}_{24}\text{O}_{72}\}$ ,  $\{\text{Nb}_{32}\text{O}_{96}\}$ , and  $\{\text{K}_{12}\text{Nb}_{96}\text{O}_{288}\}$  Clusters. *J. Am. Chem. Soc.* **2012**, 134, 14004–14010. (b) Wang, Z.-L.; Tan, H.-Q.; Chen, W.-L.; Li, Y.-G.; Wang, E.-B. A copper(II)–ethylenediamine modified polyoxoniobate with photocatalytic  $\text{H}_2$  evolution activity under visible light irradiation. *Dalton Trans.* **2012**, 41, 9882–9884.



- (3) (a) Fielden, J.; Sumliner, J. M.; Han, N.; Geletii, Y. V.; Xiang, X.; Musaev, D. G.; Lian, T.; Hill, C. L. Water splitting with polyoxometalate-treated photoanodes: enhancing performance through sensitizer design. *Chem. Sci.* **2015**, *6*, 5531–5543. (b) Liu, Y. P.; Zhao, S. F.; Guo, S. X.; Bond, A. M.; Zhang, J.; Zhu, G.; Geletii, Y. V.; Hill, C. L. Electrooxidation of Ethanol and Methanol Using the Molecular Catalyst  $[\{\text{Ru}_4\text{O}_4(\text{OH})_2(\text{H}_2\text{O})_4\}(\gamma\text{-SiW}_{10}\text{O}_{36})_2]^{10-}$ . *J. Am. Chem. Soc.* **2016**, *138*, 2617–2628.
- (4) Niu, L.; Ma, P.; Niu, H.; Li, J.; Zhao, J.; Song, Y.; Wang, J. Giant Polyniobate Clusters Based on  $[\text{Nb}_7\text{O}_{22}]^{9-}$  Units Derived from a  $\text{Nb}_6\text{O}_{19}$  Precursor. *Chem. - Eur. J.* **2007**, *13*, 8739–8748.
- (5) Tsunashima, R.; Long, D.-L.; Miras, H. N.; Gabb, D.; Pradeep, C. P.; Cronin, L. The Construction of High-Nuclearity Isopolyoxoniobates with Pentagonal Building Blocks:  $[\text{H}\text{Nb}_{27}\text{O}_{76}]^{16-}$  and  $[\text{H}_{10}\text{Nb}_{31}\text{O}_{93}(\text{CO}_3)]^{23-}$ . *Angew. Chem., Int. Ed.* **2010**, *49*, 113–116.
- (6) (a) Ikeya, T.; Senna, M. J. Change in the structure of niobium pentoxide due to mechanical and thermal treatments. *J. Non-Cryst. Solids* **1988**, *105*, 243–250. (b) Kato, K.; Tamura, S. Die kristallstruktur von  $\text{T-Nb}_2\text{O}_5$ . *Acta Crystallogr., Sect. B: Struct. Crystallogr. Cryst. Chem.* **1975**, *B31*, 673–677.
- (7) (a) Müller, A.; Das, S. K.; Fedin, V. P.; Krickemeyer, E.; Beugholt, C.; Bögge, H.; Schmidtman, M.; Hauptfleisch, B. Rapid and Simple Isolation of the Crystalline Molybdenum-Blue Compounds with Discrete and Linked Nanosized Ring-Shaped Anions:  $\text{Na}_3\text{Mo}_{126}^{\text{VI}}\text{Mo}_{28}^{\text{VO}}\text{O}_{462}\text{H}_{14}(\text{H}_2\text{O})_{700.5}$   $\text{Mo}_{124}^{\text{VI}}\text{Mo}_{28}^{\text{VO}}\text{O}_{457}\text{H}_{14}(\text{H}_2\text{O})_{680}$ . *S. C. A. 4.00 H<sub>2</sub>O* and  $\text{Na}_{22}\text{Mo}_{118}^{\text{VI}}\text{Mo}_{28}^{\text{VO}}\text{O}_{442}\text{H}_{14}(\text{H}_2\text{O})_{58}\text{CA.250H}_2\text{O}$ . *Z. Anorg. Allg. Chem.* **1999**, *625*, 1187–1192. (b) Müller, A.; Krickemeyer, E.; Bögge, H.; Schmidtman, M.; Peters, F. Organizational Forms of Matter: An Inorganic Super Fullerene and Keplerate Based on Molybdenum Oxide. *Angew. Chem., Int. Ed.* **1998**, *37*, 3359–3363.
- (8) Flynn, C. M.; Stucky, G. D. Sodium 6-niobo(ethylenediamine)-cobaltate(III) and its chromate(III) analog. *Inorg. Chem.* **1969**, *8*, 178–180.
- (9) Sheldrick, G. M. Crystal structure refinement with SHELXL. *Acta Crystallogr., Sect. C: Struct. Chem.* **2015**, *C71*, 3–8.
- (10) Hübschle, C. B.; Sheldrick, G. M.; Ditttrich, B. ShelXle: a Qt graphical user interface for SHELXL. *J. Appl. Crystallogr.* **2011**, *44*, 1281–1284.
- (11) APEX2 (Version 1.08), SAINT (Version 7.03), and SADABS (Version 2.11), Bruker Advanced X-ray Solutions; Bruker AXS Inc.: Madison, WI, 2004.
- (12) Pope, M. T. *Heteropoly and Isopolyoxometalates*; Springer-Verlag: Berlin, 1983.
- (13) Nyman, M.; Bonhomme, F.; Alam, T. M.; Rodriguez, M. A.; Cherry, B. R.; Krumhansl, J. L.; Nenoff, T. M.; Sattler, A. M. A General Synthetic Procedure for Heteropoly-niobates. *Science* **2002**, *297*, 996–998.
- (14) Nyman, M.; Bonhomme, F.; Alam, T. M.; Parise, J. B.; Vaughan, G. M. B.  $[\text{SiNb}_{12}\text{O}_{40}]^{16-}$  and  $[\text{GeNb}_{12}\text{O}_{40}]^{16-}$ : Highly Charged Keggin Ions with Sticky Surfaces. *Angew. Chem., Int. Ed.* **2004**, *43*, 2787–2792.
- (15) Bonhomme, F.; Larentzos, J. P.; Alam, T. M.; Maginn, E. J.; Nyman, M. Synthesis, Structural Characterization, and Molecular Modeling of Dodecaniobate Keggin Chain Materials. *Inorg. Chem.* **2005**, *44*, 1774–1785.
- (16) Hou, Y.; Zakharov, L. N.; Nyman, M. Observing assembly of complex inorganic materials from polyoxometalate building blocks. *J. Am. Chem. Soc.* **2013**, *135*, 16651–16657.
- (17) (a) Kato, R.; Kobayashi, A.; Sasaki, Yu. 1:14 Heteropolyvanadate of phosphorus: preparation and structure. *J. Am. Chem. Soc.* **1980**, *102*, 6571–6572. (b) Kato, R.; Kobayashi, A.; Sasaki, Yu. The heteropolyvanadate of phosphorus. Crystallographic and NMR studies. *Inorg. Chem.* **1982**, *21*, 240–246.
- (18) Bakri, R.; Booth, A.; Harle, G.; Middleton, P. S.; Wills, C.; Clegg, W.; Harrington, R. W.; Errington, R. J. Rational addition of capping groups to the phosphomolybdate Keggin anion  $[\text{PMo}_{12}\text{O}_{40}]^{3-}$  by mild, non-aqueous reductive aggregation. *Chem. Commun.* **2012**, *48*, 2779–2781.
- (19) Sha, J. Q.; Peng, J.; Tian, A. X.; Liu, H. S.; Chen, J.; Zhang, P. P.; Su, Z. M. Assembly of Multitrack Cu–N Coordination Polymeric Chain-Modified Polyoxometalates Influenced by Polyoxoanion Cluster and Ligand. *Cryst. Growth Des.* **2007**, *7*, 2535–2541.
- (20) (a) Lehmann, J.; Gaita-Ario, A.; Coronado, E.; Loss, D. Spin qubits with electrically gated polyoxometalate molecules. *Nat. Nanotechnol.* **2007**, *2*, 312–317. (b) Long, D.-L.; Tsunashima, R.; Cronin, L. Polyoxometalates: building blocks for functional nanoscale systems. *Angew. Chem., Int. Ed.* **2010**, *49*, 1736–1758.
- (21) Son, J.-H.; Ohlin, C. A.; Larson, E. C.; Yu, P.; Casey, W. H. Synthesis and Characterization of a Soluble Vanadium-Containing Keggin Polyoxoniobate by ESI-MS and  $^{51}\text{V}$  NMR:  $(\text{TMA})_9[\text{V}_3\text{Nb}_{12}\text{O}_{42}]\cdot 18\text{H}_2\text{O}$ . *Eur. J. Inorg. Chem.* **2013**, *2013*, 1748–1753.
- (22) Guo, G.; Xu, Y.; Cao, J.; Hu, C. An unprecedented vanadoniobate cluster with ‘trans-vanadium’ bicapped Keggin-type  $\{\text{VNB}_{12}\text{O}_{40}(\text{VO})_2\}$ . *Chem. Commun.* **2011**, *47*, 9411–9413.
- (23) Shen, J.-Q.; Zhang, Y.; Zhang, Z.-M.; Li, Y.-G.; Gao, Y.-Q.; Wang, E.-B. Polyoxoniobate-based 3D framework materials with photocatalytic hydrogen evolution activity. *Chem. Commun.* **2014**, *50*, 6017–6019.
- (24) Huang, P.; Zhou, E.-L.; Wang, X.-L.; Sun, C.-Y.; Wang, H.-N.; Xing, Y.; Shao, K.-Z.; Su, Z.-M. New heteropoly-niobates based on a bicapped Keggin-type  $\{\text{VNB}_{14}\}$  cluster with selective adsorption and photocatalytic properties. *CrystEngComm* **2014**, *16*, 9582–9585.
- (25) Hou, D.; Hagen, K. S.; Hill, C. L. Pentadecavanadate,  $\text{V}_{15}\text{O}_{42}^{9-}$ , a new highly condensed fully oxidized isopolyvanadate with kinetic stability in water. *J. Chem. Soc., Chem. Commun.* **1993**, *0*, 426–428.
- (26) (a) Rooksby, H. P.; White, E. A. D. The structures of 1:1 compounds of rare earth oxides with niobia and tantalum. *Acta Crystallogr.* **1963**, *16*, 888–890. (b) Yoshida, S.; Nishimura, Y.; Tanaka, T.; Kanai, H.; Funabiki, T. The local structures and photocatalytic activity of supported niobium oxide catalysts. *Catal. Today* **1990**, *8*, 67–75.
- (27) Tsunekawa, S.; Kamiyama, T.; Sasaki, K.; Asano, H.; Fukuda, T. Precise structure analysis by neutron diffraction for  $\text{RNbO}_4$  and distortion of  $\text{NbO}_4$  tetrahedra. *Acta Crystallogr., Sect. A: Found. Crystallogr.* **1993**, *A49*, 595–600.
- (28) Fulle, K.; McMillen, C. D.; Sanjeewa, L. D.; Kolis, J. W. Hydrothermal Chemistry and Growth of Fergusonite-type  $\text{RENbO}_4$  ( $\text{RE} = \text{La-Lu}$ , Y) Single Crystals and New Niobate Hydroxides. *Cryst. Growth Des.* **2016**, *16*, 4910–4917.
- (29) Subramanian, M. A.; Aravamudan, G.; Rao, G. V. S. Oxide pyrochlores—A review. *Prog. Solid State Chem.* **1983**, *15*, 55–143.
- (30) Lv, Y.; Willkomm, J.; Leskes, M.; Steiner, A.; King, T. C.; Gan, L.; Reisner, E.; Wood, P. T.; Wright, D. S. Formation of  $\text{Ti}_{28}\text{Ln}$  Cages, the Highest Nuclearity Polyoxotitanates ( $\text{Ln} = \text{La, Ce}$ ). *Chem. - Eur. J.* **2012**, *18*, 11867–11870.
- (31) Hardcastle, F. D.; Wachs, I. E. Determination of niobium-oxygen bond distances and bond orders by Raman spectroscopy. *Solid State Ionics* **1991**, *45*, 201–213.